# Off-resonant-mode instabilities in mixed absorptive and dispersive optical bistability

M. L. Asquini and L. A. Lugiato
*Dipartimento di Fisica, Università di Milano, via Celoria 16, 20133 Milano, Italy*

H. J. Carmichael
*Department of Physics, University of Arkansas, Fayetteville, Arkansas 72701*

L. M. Narducci
*Department of Physics and Atmospheric Science, Drexel University, Philadelphia, Pennsylvania 19104*
(Received 16 April 1985)

We analyze instabilities in mixed absorptive and dispersive optical bistability in the rate-equation approximation and the mean-field and good-cavity limits. Our starting point is a set of multimode equations derived from the Maxwell-Bloch equations for ring-cavity boundary conditions. We obtain analytic expressions for the instability conditions. In a plane-wave analysis, we find that a portion of the lower transmission branch can be unstable in addition to the upper-branch instability found in purely absorptive bistability. Also, a new disconnected region of instability can exist on the upper branch. Our analysis becomes particularly simple for equal and opposite cavity detunings and we explore this case in detail. We extend our treatment to include a Gaussian transverse intensity profile and show that the instabilities remain in the presence of Gaussian averaging. We also show that many of the results obtained in the rate-equation approximation hold when the atomic linewidth and atomic decay rate are of the same order.

## I. INTRODUCTION

Optical systems are very appropriate for the study of instabilities, self-pulsing, and chaotic behavior. One particular advantage they have over hydrodynamic systems, for example, is that cavities can be used to tailor the mode structure of the optical fields. One can then deal with tractable theories involving just a few modes and still expect good agreement with experiments.

The study of instabilities in optical bistability[1] (OB) was initiated in work by McCall[2] and Bonifacio and Lugiato.[3] The analysis in Ref. 3 is based on the ring-cavity model for absorptive OB, formulated in terms of Maxwell-Bloch equations for a collection of homogeneously broadened two-level atoms interacting with a plane-wave field which satisfies ring-cavity boundary conditions. The incident field is exactly tuned to a cavity resonance—cavity detuning $\Theta=0$—and to the atomic line center—atomic detuning $\Delta=0$. Instability arises in the good-cavity limit, where the cavity linewidth $\kappa$ is much less than both the atomic linewidth $\gamma_\perp$ and longitudinal relaxation rate $\gamma_\parallel$, provided the nearest nonresonant cavity modes are detuned from the incident laser by less than the Rabi frequency. Along part of the upper branch of the hysteresis cycle, a set of off-resonance cavity modes, symmetrically placed with respect to the resonant mode, are unstable and undamped self-pulsing arises. In the mean-field limit, the pulsation period is of the order of the cavity round-trip time $t_R$, corresponding to a beat frequency determined by the longitudinal mode spacing in the empty cavity; the mean-field limit is defined with $\alpha L \ll 1$, $T \ll 1$, and $\alpha L/T$ arbitrary, where $\alpha$ is the unsaturated absorption coefficient, $L$ is the length of the atomic sample, and $T$ is the mirror transmission coefficient. Outside the mean-field limit, the pulsing frequency is renormalized by the atom-field interaction, but remains of the order of $t_R^{-1}$.[4]

For the general case $\Delta\neq 0$, $\Theta\neq 0$, the ring-cavity model of OB is analyzed in Ref. 5 after adiabatic elimination of the polarization (rate-equation approximation). This requires $\gamma_\perp \gg \gamma_\parallel$ and $\gamma_\perp \gg 2\pi/t_R$, where the second inequality requires the free spectral range to be much less than the atomic linewidth. Under these conditions, the ring-cavity model can be formulated as a set of differential difference equations.[5] If the free spectral range is also much smaller than the longitudinal decay rate, $\gamma_\parallel \gg 2\pi/t_R$, the model simplifies to a two-dimensional discrete map. Then, when the steady state becomes unstable, all cavity modes are simultaneously unstable, and spontaneous pulsations arise with a period equal to twice the cavity round-trip time. The first prediction of chaotic behavior in OB was made for this model.[5,6] By suitably varying the incident intensity, the pulsation at twice the round-trip time period doubles to chaos. This behavior was first seen experimentally in a hybrid electro-optic device[7] and more recently has been seen in all-optical systems under transient conditions.[8,9]

The relationship between the results of Refs. 3 and 4 and those of Refs. 5 and 6 has been discussed by Lugiato *et al.*[10] and Carmichael.[11] In the mean-field limit, pulsations of period $2t_R$ arise when the incident field is tuned midway between adjacent cavity resonances. In Ref. 11 it is shown that the eigenvalues of the linearized stability analysis for a cavity tuned to resonance (Refs. 3 and 4) and for a cavity tuned between resonances (Refs. 5 and 6) are related by a simple symmetry. Many other papers have studied these and related instabilities; see especially

 

Refs. 12–16.

In each of the instabilities mentioned above, two or more off-resonant modes become unstable. A second class of instabilities in OB exists where only the mode nearest resonance with the incident field becomes unstable. This instability requires that either $\Delta$ or $\Theta$, or both, be nonzero. This resonant-mode instability was found by Ikeda and Akimoto[17] in a Kerr medium model and by Lugiato *et al.*[18] for two-level atoms. In the mean-field limit, instability arises when the atomic longitudinal relaxation rate is of the same order as the cavity linewidth, and therefore much less than the free spectral range, $\gamma_{\parallel} \sim \kappa \ll 2\pi/t_R$. The period of the resulting oscillations is of the order of the inverse cavity linewidth. It has been shown that oscillatory behavior is experimentally accessible provided the detunings $\Delta$ and $\Theta$ have opposite signs,[19,20] an unfavorable condition for bistability, but a favorable one for the resonant-mode instability, and as will be seen, also for the instability discussed in the present work. Recently, the resonant-mode instability has been seen in an experimental system using multiple atomic beams.[21]

In this paper, we are concerned with off-resonant-mode instabilities in OB for the general case of mixed absorptive and dispersive bistability, and the mean-field and good-cavity limits. We start from the Maxwell-Bloch equations for a ring cavity and a collection of homogeneously broadened two-level atoms. Our first aim is to extend the plane-wave theory of Refs. 3 and 4 to include $\Delta \neq 0$, $\Theta \neq 0$. Analytic formulas for the eigenvalues of the linear stability analysis for the general values of $\Delta$ and $\Theta$ have previously been obtained,[13] however, they are very complicated and give little insight into the overall picture of the instability domain. Here, we will adopt the rate-equation approximation, with the polarization adiabatically eliminated. We then obtain relatively simple conditions defining the regions of instability. In particular, we find that $\Theta = -\Delta$ provides an especially simple case for which we obtain analytic formulas for the instability domain. For general values of $\Delta$ and $\Theta$, we find two notable new features compared with the results for purely absorptive OB. First, instability can extend to a portion of the lower branch of the hysteresis loop, and, second, a new disconnected region of instability can appear on the upper branch. It has already been noted in Ref. 12 that for $\Delta \neq 0$, $\Theta \neq 0$ instability can occur in the absence of bistability. In addition to analyzing the instability domain, we derive a set of equations suitable for the numerical calculation of the self-pulsing solutions when only the first pair of off-resonant modes are unstable. Using a simplified version[22,23] of the dressed-mode formalism of OB (Refs. 24 and 25) we reduce the full Maxwell-Bloch equations, which are partial differential equations in space and time, to a set of six ordinary differential equations in time.

Our second aim in this paper is to analyze the effect of the transverse intensity variation in a laser beam on these off-resonant-mode instabilities. We consider a ring cavity with spherical mirrors and assume that the incident beam is matched to the $TEM_{00}$ mode of the cavity. Under appropriate conditions, specified below, it is reasonable to assume that the beam preserves its Gaussian transverse profile in the presence of the atom-field interaction. We describe the system by a set of dynamical equations that include all longitudinal cavity modes, but only one transverse mode. The off-resonant-mode instability in absorptive OB, $\Delta = \Theta = 0$ has been analyzed using this model by Lugiato and Milani.[26] They show that the extension of the instability domain is governed by the ratio $d/W_0$, where $d$ is the radius of the cylindrical atomic sample and $W_0$ is the beam waist. In the limit $d/W_0 \to 0$, the plane-wave theory is recovered, whereas for $d/W_0 \gg 1$ the off-resonant-mode instability is completely destroyed by the radial Gaussian averaging.[26,27] In contrast, the resonant-mode instability survives for $d/W_0 \gg 1$.[20] Here we analyze the effect of Gaussian averaging on the off-resonant-mode instability for general values of $\Delta$ and $\Theta$. We find that all instabilities—instability on the lower and upper branch of the hysteresis loop, the disconnected range of instability on the upper branch, and instability in the absence of bistability—persist for $d/W_0 \gg 1$.

In Sec. II we derive the plane-wave mode equations from the Maxwell-Bloch equations after adiabatic elimination of the polarization. These equations are linearized around the steady state in Sec. III and the resulting eigenvalues governing the stability of the steady state are analyzed in Sec. IV. In Sec. V we focus on the special case $\Theta = -\Delta$. In Sec. VI we derive a closed set of nonlinear differential equations for the field variables by adiabatically eliminating the atomic inversion. The stability analysis for a Gaussian transverse intensity profile is given in Sec. VII, and results are compared with those from the plane-wave theory. Concluding discussion in Sec. VIII shows that most of the results obtained in the rate-equation limit also hold for $\gamma_{\parallel} \approx \gamma_{\perp}$.

## II. DERIVATION OF MODE EQUATIONS WITH ADIABATIC ELIMINATION OF THE ATOMIC POLARIZATION

We consider a ring cavity of length $\mathscr{L}$ containing a two-level homogeneously broadened atomic sample of length $L$. Coupled Maxwell-Bloch equations describe propagation of the electric field through the atomic sample. In the plane-wave and slowly varying amplitude approximations, these can be cast into the following form [for details, see Ref. 1(c)]:

$$\frac{\partial F}{\partial t} + c\frac{\partial F}{\partial z} = -\alpha c P \ , \tag{1a}$$

$$\frac{\partial P}{\partial t} = \gamma_{\perp}[FD - P(1 + i\Delta)] \ , \tag{1b}$$

$$\frac{\partial D}{\partial t} = \gamma_{\parallel}[\tfrac{1}{2}(FP^* + F^*P) + D - 1] \ , \tag{1c}$$

where $F$, $P$, and $D$ are suitably defined dimensionless variables corresponding to the field amplitude, the atomic polarization, and the atomic population difference between the lower and the upper states, respectively; $\alpha$ is the unsaturated resonant absorption coefficient for the field amplitude; $\gamma_{\parallel} = T_1^{-1}$ and $\gamma_{\perp} = T_2^{-1}$ are the longitudinal and transverse atomic relaxation rates, and

$$\Delta = (\omega_a - \omega_0)/\gamma_{\perp} \ , \tag{2}$$

where $\omega_a$ is the atomic transition frequency and $\omega_0$ is the frequency of the field. In the presence of the cavity, Eqs. (1) are to be solved subject to the boundary condition

$$F(0,t)=TY+(1-T)e^{-i\Theta T}F(L,t-(\mathscr{L}-L)/c)\ , \tag{3}$$

where $T$ is the transmission coefficient of the input and output mirrors, $Y$ is the dimensionless input field amplitude, and

$$\Theta=(\omega_c-\omega_0)/\kappa\ , \tag{4}$$

where $\omega_c$ is the frequency of the nearest cavity resonance and

$$\kappa=cT/\mathscr{L}=Tt_R^{-1} \tag{5}$$

is the cavity linewidth.

In this paper, we make two further simplifications of Eqs. (1). First, we treat only the mean-field limit

$$\alpha L\ll 1,\quad T\ll 1\ , \tag{6a}$$

with

$$C=\frac{\alpha L}{2T}\quad\text{and}\quad\Theta\ \text{arbitrary}\ , \tag{6b}$$

where Eqs. (1) may be reexpressed in the form[1(c),24]

$$\frac{\partial F}{\partial t'}+c\frac{L}{\mathscr{L}}\frac{\partial F}{\partial z}=-\kappa[(1+i\Theta)F+2CP-Y]\ , \tag{7a}$$

$$\frac{\partial P}{\partial t'}=\gamma_\perp[FD-(1+i\Delta)P]\ , \tag{7b}$$

$$\frac{\partial D}{\partial t'}=-\gamma_{||}[\tfrac{1}{2}(FP^*+F^*P)+D-1]\ , \tag{7c}$$

with

$$t'=t+\frac{\mathscr{L}-L}{c}\frac{z}{L}\ , \tag{8}$$

where $F$ now satisfies the standard periodic boundary condition

$$F(0,t')=F(L,t')\ . \tag{9}$$

Second, for

$$\gamma_\perp\gg\gamma_{||},\quad\gamma_\perp\gg\frac{c}{\mathscr{L}}=t_R^{-1} \tag{10}$$

we adiabatically eliminate the atomic polarization setting $\partial P/\partial t'=0$ and solve Eq. (7b) for $P$ in terms of the more slowly varying quantities $F$ and $D$. This corresponds to the well-known rate-equation approximation. Equations (7) are then replaced by

$$\frac{\partial\bar F}{\partial t'}+c\frac{L}{\mathscr{L}}\frac{\partial\bar F}{\partial z}=-\kappa[(1+i\Theta)\bar F+2\bar C(1-i\Delta)\bar F D-\bar Y]\ , \tag{11a}$$

$$\frac{\partial D}{\partial t'}=-\gamma_{||}[(1+|\bar F|^2)D-1]\ , \tag{11b}$$

where

$$\bar F=F/(1+\Delta^2)^{1/2},\quad\bar Y=Y/(1+\Delta^2)^{1/2}\ ,\quad\bar C=C/(1+\Delta^2)\ . \tag{12}$$

The transformation leading from Eqs. (1) to (7) conveniently recasts Eq. (3) as a standard periodic boundary condition and isolates all terms proportional to $T\ll 1$ in $\kappa=Tt_R^{-1}$ on the right-hand side (rhs) of Eq. (11a). For $\kappa=0$, the solutions to Eqs. (11a) and (9) are plane traveling waves with wave vectors

$$k_n=\frac{2\pi n}{L},\quad n=0,\pm1,\pm2,\ldots \tag{13a}$$

and frequencies

$$\alpha_n=k_n\left[c\frac{L}{\mathscr{L}}\right]=2\pi n t_R^{-1} \tag{13b}$$

corresponding to longitudinal modes with frequencies $\omega_0+\alpha_n$ for an empty cavity with perfect reflectors. Note that

$$k_nz-\alpha_nt'=\left[\frac{L}{\mathscr{L}}k_n\right]z-\alpha_nt=\frac{2\pi n}{\mathscr{L}}(z-ct)\ .$$

Then, for $\kappa\neq0$, we introduce the mode expansion

$$\left.\begin{matrix}\bar F(z,t')\\ D(z,t')\end{matrix}\right\}=\sum_n e^{i(k_nz-\alpha_nt')}\times\left\{\begin{matrix}f_n(t')\\ d_n(t')\end{matrix}\right. \tag{14}$$

and after substituting in Eqs. (7) the mode amplitudes $f_n$ and $d_n$ satisfy (the overdot signifies $d/dt'$)

$$\dot f_n=-\kappa\left[(1+i\Theta)f_n+2\bar C(1-i\Delta)\sum_{n'}f_{n'}d_{n-n'}-\bar Y\delta_{n,0}\right]\ , \tag{15a}$$

$$\dot d_n=i\alpha_nd_n-\gamma_{||}\left[d_n+\sum_{n',n''}f_{n'}^*f_{n''}d_{n+n'-n''}-\delta_{n,0}\right]\ . \tag{15b}$$

Also, $f_n^*$ satisfies the complex conjugate of Eq. (15a) and since $D$ must be real, $d_n^*=d_{-n}$.

The steady-state solution of Eqs. (11) obtained by setting

$$\frac{\partial F}{\partial t'}=\frac{\partial D}{\partial t'}=0$$

and imposing the boundary condition Eq. (9), is uniform in space. Then only $f_0$ and $d_0$ are nonzero in the steady-state solution of Eqs. (15). This steady state is given by

$$f_n^{(\mathrm{st})}=d_n^{(\mathrm{st})}=0\ \text{ for } n\neq0\ , \tag{16}$$

$$f_0^{(\mathrm{st})}=Xe^{i\phi_x}=X\left[\frac{(1-i\Theta)(1+X^2)+2\bar C(1+i\Delta)}{(1+i\Theta)(1+X^2)+2\bar C(1-i\Delta)}\right]^{1/2}\ , \tag{17a}$$

$$d_0^{(\mathrm{st})}=\frac{1}{1+X^2}\ , \tag{17b}$$

where $X=|f_0^{(\mathrm{st})}|$ satisfies the familiar state equation[1(c)]

$$\bar Y=X\left[\left[1+\frac{2\bar C}{1+X^2}\right]^2+\left[\Theta-\frac{2\bar C\Delta}{1+X^2}\right]^2\right]^{1/2}\ . \tag{18}$$

## III. LINEAR STABILITY ANALYSIS

To check the stability of the steady state, we write

$$f_n = f_n^{(\mathrm{st})} + \delta f_n \ , \qquad d_n = d_n^{(\mathrm{st})} + \delta d_n \ , \tag{19}$$

and substitute in Eqs. (15) retaining only linear terms in the perturbations $\delta f_n$ and $\delta d_n$. Taking Eq. (16) into account, for each $n$ we find the set of three equations coupling $\delta f_n$, $\delta f^*_{-n}$, and $\delta d_n$

$$\dot{\delta} f_n = -\kappa[(1+i\Theta)\delta f_n + 2\bar{C}(1-i\Delta)(f_0^{(\mathrm{st})}\delta d_n + d_0^{(\mathrm{st})}\delta f_n)] \ , \tag{20a}$$

$$\dot{\delta} f^*_{-n} = -\kappa[(1-i\Theta)\delta f^*_{-n} + 2\bar{C}(1+i\Delta)(f_0^{(\mathrm{st})*}\delta d_n + d_0^{(\mathrm{st})}\delta f^*_{-n})] \ , \tag{20b}$$

$$\dot{\delta} d_n = i\alpha_n \delta d_n - \gamma_{\parallel}[(1+|f_0^{(\mathrm{st})}|^2)\delta d_n + d_0^{(\mathrm{st})}(f_0^{(\mathrm{st})*}\delta f_n + f_0^{(\mathrm{st})}\delta f^*_{-n})] \ . \tag{20c}$$

We are interested in off-resonant-mode instabilities which arise in the limit[15(c)]

$$\gamma_{\parallel} \gg \kappa \ . \tag{21}$$

We, therefore, adiabatically eliminate the variables $\delta d_n$, setting $\dot{\delta} d_n = 0$ in Eq. (20c) and solving for $\delta d_n$ in terms of $\delta f_n$ and $\delta f^*_{-n}$. This is quite different from the adiabatic elimination of $P$ at the level of Eqs. (11). There we assume that $P$ can follow a self-pulsing frequency $\sim t_R^{-1}$ [Eq. (10)]. Here we require only $\gamma_{\parallel} \gg \kappa = T t_R^{-1} \ll t_R^{-1}$. After substituting for $\delta d_n$ into Eqs. (20a) and (20b) and introducing the steady-state solution from Eqs. (17), we obtain

$$\kappa^{-1}\frac{d}{dt'}\delta f'_n = -\left[(1+i\Theta)+(1-i\Delta)\frac{2\bar{C}}{1+X^2}\frac{1-i\tilde{\alpha}}{1+X^2-i\tilde{\alpha}_n}\right]\delta f'_n + (1-i\Delta)\frac{2\bar{C}}{1+X^2}\frac{X^2}{1+X^2-i\tilde{\alpha}_n}\delta f'^*_{-n} \ , \tag{22a}$$

$$\kappa^{-1}\frac{d}{dt'}\delta f'^*_{-n} = -\left[(1-i\Theta)+(1+i\Delta)\frac{2\bar{C}}{1+X^2}\frac{1-i\tilde{\alpha}}{1+X^2-i\tilde{\alpha}_n}\right]\delta f'^*_{-n} + (1+i\Delta)\frac{2\bar{C}}{1+X^2}\frac{X^2}{1+X^2-i\tilde{\alpha}_n}\delta f'_n \ , \tag{22b}$$

where

$$\delta f'_n = e^{-i\phi_x}\delta f_n, \quad \delta f'^*_{-n} = e^{i\phi_x}\delta f^*_{-n} \ , \tag{23}$$

and

$$\tilde{\alpha}_n = \alpha_n/\gamma_{\parallel} = 2\pi n(\gamma_{\parallel} t_R)^{-1} \ . \tag{24}$$

These equations have exponential solutions

$$\begin{bmatrix} \delta f'_n(t') \\ \delta f'^*_{-n}(t') \end{bmatrix} = e^{\lambda_n(\kappa t')}\begin{bmatrix} \delta f'_n(0) \\ \delta f'^*_{-n}(0) \end{bmatrix} \ , \tag{25}$$

where the eigenvalues $\lambda_n$ must satisfy the equation

$$\lambda_n^2 + 2\lambda_n\left[1+\frac{2\bar{C}}{1+X^2}\frac{1-i\tilde{\alpha}_n}{1+X^2-i\tilde{\alpha}_n}\right] + \left[1+\frac{2\bar{C}}{1+X^2}\right]\left[1+\frac{2\bar{C}}{1+X^2}\frac{1-X^2-i\tilde{\alpha}_n}{1+X^2-i\tilde{\alpha}_n}\right] + \left[\Theta-\frac{2\bar{C}}{1+X^2}\right]\left[\Theta-\frac{2\bar{C}\Delta}{1+X^2}\frac{1-X^2-i\tilde{\alpha}_n}{1+X^2-i\tilde{\alpha}_n}\right] = 0 \ . \tag{26}$$

Equation (26) is a special case of the eigenvalue equation derived in Ref. 13. The solutions given in Eqs. (19) and (20) of Ref. 13 require $\gamma_{\perp} \sim \gamma_{\parallel} \gg \kappa$ rather than $\gamma_{\perp} \gg \gamma_{\parallel} \gg \kappa$ [Eqs. (10) and (21)] and therefore depend on both $\gamma_{\parallel}$ and $\gamma_{\perp}$. If the limit $\gamma_{\perp} \gg \alpha_n$, $\gamma_{\perp} \gg \gamma_{\parallel}$, with $\tilde{\alpha}_n = \alpha_n/\gamma_{\parallel}$ arbitrary, is taken in these equations the solutions of Eq. (26) are recovered. Equation (26) is also a special case of the eigenvalue equation derived in Refs. 15(b) and 15(c). Equations (2.11) in Ref. 15(b) and (2.17) in Ref. 15(c) are derived for the limit of Eq. (10) but are valid outside the mean-field limit. Equation (26) follows from these equations in the limit of Eqs. (6) and (21).[15(c)]

## IV. ANALYSIS OF THE EIGENVALUE EQUATION

For each value of $n$, Eq. (26) determines the stability of the cavity mode with frequency $\omega_0 + \alpha_n = \omega_0 + 2\pi n t_R^{-1}$ as a function of the four parameters $\bar{C}$, $\Delta$, $\Theta$, and $(\gamma_{\parallel} t_R)^{-1}$ and the steady-state field amplitude $X$. With $\bar{C}$, $\Delta$, $\Theta$, and $X$ fixed, the corresponding input amplitude $\bar{Y}$ is determined by Eq. (18). Clearly, the stability of all modes, in all steady states, can be deduced from a study of the roots $\lambda_+(\bar{C},\Delta,\Theta,\tilde{\alpha},X)$ and $\lambda_-(\bar{C},\Delta,\Theta,\tilde{\alpha},X)$ to the quadratic equation obtained by dropping the subscript $n$ in Eq. (26). Here $\tilde{\alpha}$ is a continuous variable which plays the fol-

lowing dual role.

(1) For a particular mode (fixed $n$) the behavior of $\lambda_\pm$ as a function of $\tilde{\alpha}=2\pi n(\gamma_{\|}t_R)^{-1}$ tells us the stability of that mode as a function of cavity length and population decay rate, i.e., as a function of $(\gamma_{\|}t_R)^{-1}$.

(2) For a given cavity and atomic sample [fixed $(\gamma_{\|}t_R)^{-1}$], the behavior of $\lambda_\pm$ at the discrete values $\tilde{\alpha}=2\pi n(\gamma_{\|}t_R)^{-1}$, $n=0,\pm1,\pm2,\ldots$, tells us the stability of all the cavity modes. If we now identify regions of $(\bar{C},\Delta,\Theta,\tilde{\alpha},X)$ space for which either $\mathrm{Re}(\lambda_+)>0$ or $\mathrm{Re}(\lambda_-)>0$, then for chosen values of $C$, $\Delta$, $\Theta$, $(\gamma_{\|}t_R)^{-1}$, and $X$ all cavity modes with frequencies $\omega_0+2\pi n t_R^{-1}$ such that $(\bar{C},\Delta,\Theta,2\pi n(\gamma_{\|}t_R)^{-1},X)$ lies inside that region will be unstable. Considering off-resonant modes, this may be zero, two, four, or many modes, depending on the value of $(\gamma_{\|}t_R)^{-1}$. Alternatively, given such a region, each off-resonant mode will be unstable over some range of $(\gamma_{\|}t_R)^{-1}$. In this section, we look for regions of instability by identifying their boundaries defined by either $\mathrm{Re}(\lambda_+)=0$ or $\mathrm{Re}(\lambda_-)=0$.

We drop the subscript $n$ in Eq. (26) and look for solutions

$$\lambda=iv\ . \tag{27}$$

After substituting this solution, we obtain two equations from the requirement that the real and imaginary parts of the resulting expression vanish separately. Solving one of these to eliminate $\tilde{\alpha}$ we find

$$\tilde{\alpha}=2v\left[1+X^2+\frac{2\bar{C}}{1+X^2}\right](v^2-\bar{Y}^2/X^2)^{-1}\ , \tag{28}$$

and, from the second, $v^2$ satisfies a quadratic equation with solutions

$$v_\pm^2=g(\bar{C},\Delta,\Theta,X)\pm[\mathscr{D}(\bar{C},\Delta,\Theta,X)]^{1/2}\ , \tag{29}$$

where

$$g(\bar{C},\Delta,\Theta,X)=\left[\Theta-\frac{2\bar{C}\Delta}{1+X^2}\right]\left[\Theta-\frac{2\bar{C}\Delta}{(1+X^2)^2}\right]-\left[1+\frac{2\bar{C}}{1+X^2}\right]\left[1+\frac{2\bar{C}}{(1+X^2)^2}\right], \tag{30}$$

and

$$\mathscr{D}(\bar{C},\Delta,\Theta,X)=g(\bar{C},\Delta,\Theta,X)^2-\frac{\bar{Y}^2}{X^2}\frac{d(\bar{Y}^2)}{d(X^2)}\ . \tag{31}$$

From Eq. (18) we have

$$\frac{d(\bar{Y}^2)}{d(X^2)}=\left[1+\frac{2\bar{C}}{1+X^2}\right]\left[1+\frac{2\bar{C}}{1+X^2}\frac{1-X^2}{1+X^2}\right]+\left[\Theta-\frac{2\bar{C}\Delta}{1+X^2}\right]\left[\Theta-\frac{2\bar{C}\Delta}{1+X^2}\frac{1-X^2}{1+X^2}\right]. \tag{32}$$

The boundaries of regions of instability are now defined by the requirement that solutions for $v^2$ be real and positive. A convenient strategy for exploring the multidimensional parameter space is to analyze Eq. (29) as a function of $X$ for fixed $\bar{C}$, $\Delta$, and $\Theta$. From solutions $v_\pm^2(X)$ which are real and positive, instability boundaries can be drawn in the $(X,\tilde{\alpha})$ plane using Eq. (28). In what follows, we therefore regard $\tilde{\alpha}$, $v_\pm$, $g$, $\mathscr{D}$, and $\bar{Y}$ as functions of $X$ for fixed $\bar{C}$, $\Delta$, and $\Theta$.

The properties of Eq. (29) can be classified according to the sign of the derivative $d(\bar{Y}^2)/d(X^2)$ in Eq. (31). We make the following observations.

Observation (1): If $C$, $\Delta$, and $\Theta$ satisfy the bistability conditions [Ref. 1(c), Sec. 2.1.5], Eq. (29) gives one solution $v_-^2(X_{L,U})=0$ at the turning points of the bistability curve, where $d(\bar{Y}^2)/d(X^2)=0$. Here $X_L$ and $X_U$ denote the lower-branch and upper-branch turning points, respectively. Then, for fixed $\bar{C}$, $\Delta$, and $\Theta$, $(X_L,0)$ and $(X_U,0)$ are points in the $(X,\tilde{\alpha})$ plane where instability boundaries cross the $X$ axis. For $\tilde{\alpha}=0$, Eq. (26) gives

$$\lambda_\pm=-\left[1+\frac{2\bar{C}}{(1+X^2)^2}\right]\pm\left[\left[1+\frac{2\bar{C}}{1+X^2}\right]^2-\frac{\bar{Y}^2}{X^2}\frac{d(\bar{Y}^2)}{d(X^2)}\right]^{1/2} \tag{33}$$

and clearly, the range $X_L<X<X_U$ of the $X$ axis lies inside the unstable region. Then along the negative-slope branch of the bistability curve, the resonant mode [with $n=0$, $\tilde{\alpha}_n=2\pi n(\gamma_{\|}t_R)^{-1}=0$] is unstable for all values of $(\gamma_{\|}t_R^{-1})$, and all off-resonant modes are unstable in the limit $(\gamma_{\|}t_R)^{-1}=\tilde{\alpha}_n/2\pi n\to0$.

Observation (2): If $C$, $\Delta$, and $\Theta$ satisfy the bistability conditions, Eq. (29) gives one real positive solution $v_+(X)$ throughout the range $X_L<X<X_U$ where $d(\bar{Y}^2)/d(X^2)<0$. Then for fixed $C$, $\Delta$, and $\Theta$, Eq. (28) defines two segments of the instability boundary $\tilde{\alpha}(X)$ in the $(X,\tilde{\alpha})$ plane, symmetrically placed about the $X$ axis:

$$\tilde{\alpha}(X)=\tilde{\alpha}_+(X)=\pm2|v_+(X)|\left[1+X^2+\frac{2\bar{C}}{1+X^2}\right]\times[v_+(X)-\bar{Y}(X)^2/X^2]^{-1}\ . \tag{34}$$

Since the $X$ axis lies within the unstable region, the region $X_L<X<X_U$, $|\alpha|<|\alpha_+(X)|$ of the $(X,\tilde{\alpha})$ plane is un-

stable. Then along the negative-slope branch of the bistability curve, each off-resonant mode is unstable for values of $(\gamma_{\|}t_R)^{-1}$ in the range $0 \le (\gamma_{\|}t_R)^{-1} < |\tilde{\alpha}_+(X)|/2\pi|n|$.

Observation (3): Equation (29) gives two real positive solutions if

$$g(X)>0 \text{ and } \mathscr{D}(X)>0 \tag{35a}$$

in addition to

$$g^2 > \mathscr{D} \text{ or } \frac{d(\bar{Y}^2)}{dX^2} . \tag{35b}$$

If, for fixed $\bar{C}$, $\Delta$, and $\Theta$, these conditions are met at any point along the transmission curve $\bar{Y}(X)$, a range of positive-slope instability exists which either extends beyond $X=X_L$ or $X=X_U$ onto the negative-slope branch, or exists entirely on a positive-slope branch. In any case, all boundaries $X_P$ in the positive-slope branches are solutions to the equation

$$\mathscr{D}(X_P)=0 . \tag{36}$$

Equation (36) states that $\mathscr{D}(X)\ge 0$ must fail beyond $X_P$ rather than $g(X)>0$. This follows from Eq. (31). If $g(X_P)=0$, $\mathscr{D}(X)$ must be negative in a neighborhood of $X_P$, since $d(\bar{Y}^2)/d(X^2)>0$, and this contradicts the definition of $X_P$ as lying at the boundary of an interval with $\mathscr{D}(X)>0$. Throughout such a range of positive slope, instability segments of the instability boundary $\tilde{\alpha}(X)$ in the $(X,\tilde{\alpha})$ plane are defined both by Eq. (34) and by

$$\tilde{\alpha}(X)=\tilde{\alpha}_-(X)=\pm 2|v_-(X)|\left[1+X^2+\frac{2\bar{C}}{1+X^2}\right] \times[v_-(X)^2-\bar{Y}(X)^2/X^2]^{-1} . \tag{37}$$

The region $|\tilde{\alpha}_-(X)| < |\tilde{\alpha}| < |\tilde{\alpha}_+(X)|$ of the $(X,\tilde{\alpha})$ plane is unstable. Then for some steady-state $X$ in the range of the positive-slope instability, each off-resonant mode is unstable for values of $(\gamma_{\|}t_R)^{-1}$ in the range $|\tilde{\alpha}(X)|/2\pi|n| < (\gamma_{\|}t_R)^{-1} < |\tilde{\alpha}_+(X)|/2\pi|n|$.

From this analysis of Eq. (29), instability boundaries in the $(X,\tilde{\alpha})$ plane can be drawn, depending, for a chosen $\bar{C}$, $\Delta$, and $\Theta$, on the behavior of $d(\bar{Y}^2)/d(X^2)$, $g(X)$, and $\mathscr{D}(X)$. The behavior of $d(\bar{Y}^2)/d(X^2)$ is determined by the existence, or otherwise, of bistability, for which conditions on $\bar{C}$, $\Delta$, and $\Theta$ are known [Ref. 1(c), Sec. 2.1.5]. There remains the question of positive-slope instabilities—*can Eqs. (35) be satisfied?* Note first that for $\Delta=\Theta=0$, $g(X)$ is *always* negative; therefore, we find no positive-slope instability in absorptive bistability. This is expected, since it is known that in the limit specified by Eq. (10) the instability of Ref. 3(b) disappears [see Refs. 10, 11, and 15(b)]. In addition, in the rate-equation approximation, a resonant pump induces population pulsations that produce spectral holes even in homogeneously broadened media with an accompanying reduction of the sidemode gain.

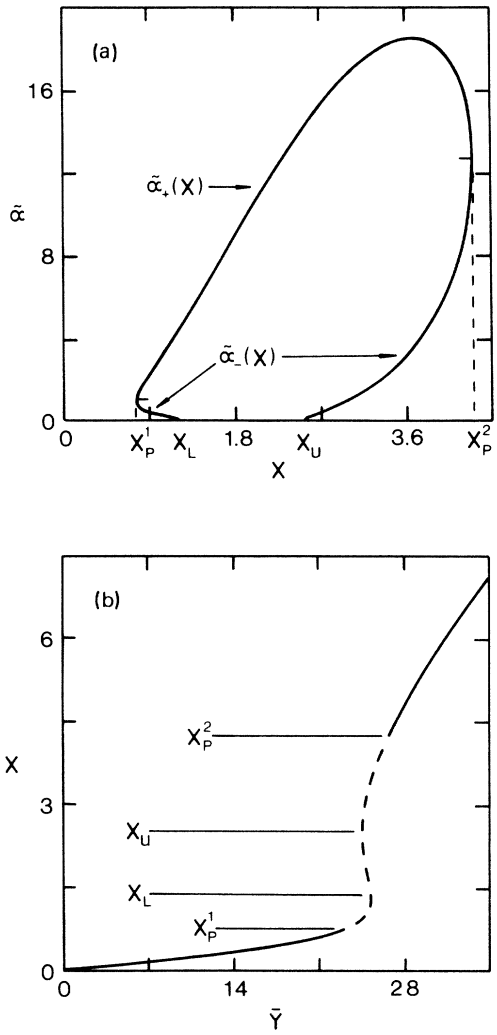


FIG. 1. (a) Instability boundary in the $(X,\tilde{\alpha})$ plane for $C=5$, $\Delta=4$, $\Theta=-4$. (b) Corresponding steady-state curve showing the unstable (dashed) line.

Next, consider the possibility that $\bar{C}$, $\Delta$, and $\Theta$, satisfying the bistability conditions, and $\Delta$ and $\Theta$ nonzero, the negative-slope instability [observation (2) above] might be contiguous with a range of instability on either the upper or lower branch. The existence of either positive-slope instability is determined by $g(X_U)$ and $g(X_L)$, respectively. Since $\mathscr{D}(X)=g(X)$ at the turning points, if $g(X_U)>0$, a range of instability must exist on the upper branch, since at $X_U$, Eq. (29) has two real positive solutions according to observation (3) above, and then the segments $\tilde{\alpha}_+(X)$ of the instability boundary in the $(X,\tilde{\alpha})$ plane, which extend through the negative-slope range $X_L<X<X_U$, do not close at $X_U$, rather the unstable region of the $(X,\tilde{\alpha})$ plane extends over a range of $X>X_U$ on the upper branch. Similarly, if $g(X_L)>0$, the unstable region of the $(X,\tilde{\alpha})$

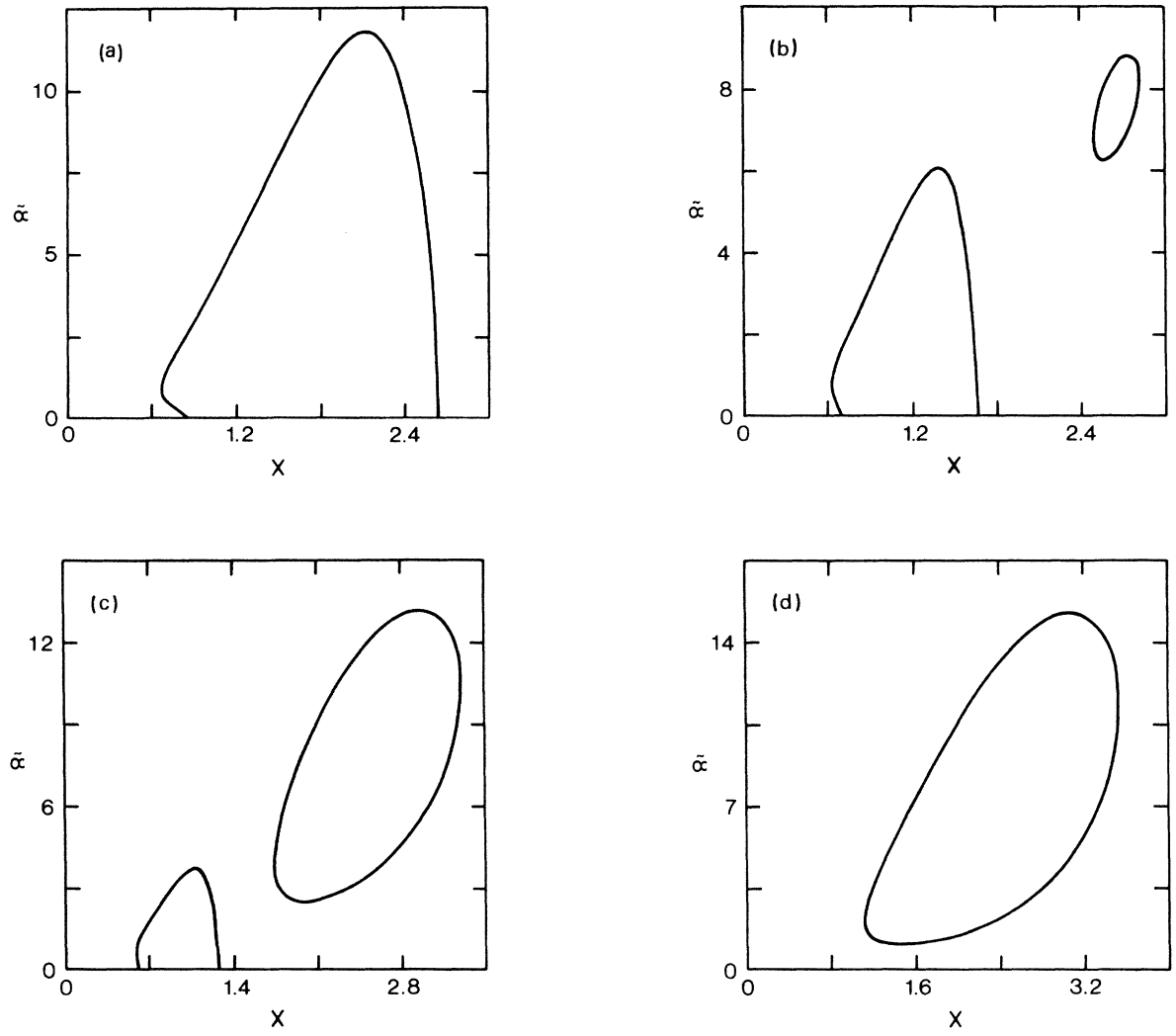


FIG. 2. Instability boundaries in the $(X,\tilde{\alpha})$ plane for $\bar{C}=4$, $\Delta=5$, and (a) $\Theta=5$, (b) $\Theta=10.5$, (c) $\Theta=15$, (d) $\Theta=30$.

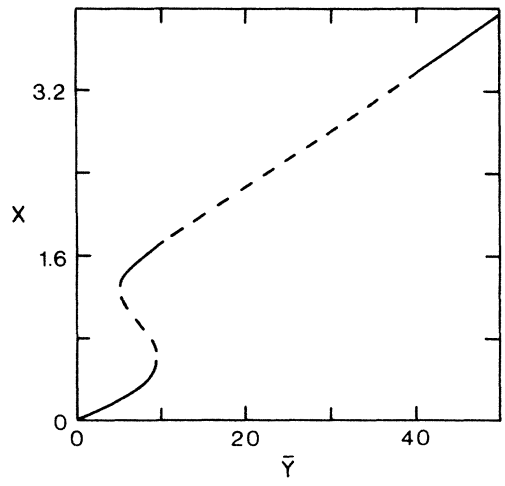


FIG. 3. Steady-state curve showing the unstable (dashed) region corresponding to Fig. 2(c).

plane extends over a range of $X<X_L$ on the lower branch. We find that both possibilities can be realized as illustrated in Fig. 1. This is quite distinct from the situation reported by Bonifacio and Lugiato[1(c),3(b)] for absorptive systems with $\gamma_{\parallel}\approx\gamma_{\perp}$, where only a portion of the upper branch could be unstable. Armbruster[28] predicted the possibility for instability on the lower branch in an analysis using imperfect bifurcation theory and suggested that it might be realized in dispersive systems. Our explicit analysis now confirms this result.

We have noted under observation (3) that every positive-slope instability must be associated with a solution $X_P$ to the equation $\mathscr{D}(X_P)=0$, more precisely, with a pair of solutions defining a range over which $\mathscr{D}(X)$ is positive. It is useful then to ask for all solutions to Eq. (36) since they are all potentially associated with positive-slope instability. Whether or not a particular $X_P$ is the boundary to a range of instability is determined by the sign of $g(X)$ in the neighborhood of $X_P$. Now $(1+X^2)^6\mathscr{D}(X)$ is a sixth-degree polynomial in $X^2$. It can

be shown that this polynomial has an even number $m \geq 2$ of real roots with $X^2 < 0$, and an even number of real roots with $X^2 > 0$. Then, for a given $\bar{C}$, $\Delta$, and $\Theta$, there are either zero, one, or two intervals of $X$ over which $\mathscr{D}(X) \geq 0$. In a bistable system, one such interval must exist since $\mathscr{D}(X)$ is always positive along the negative-slope branch. Can a second interval with $\mathscr{D}(X) \geq 0$ be realized in the positive-slope region, and, moreover, with $g(X) > 0$ so that an instability exists? We find the answer to this question is affirmative. A second unstable region can exist in the $(X,\tilde{\alpha})$ plane as illustrated in Fig. 2. Figure 2(a) illustrates a situation which is bistable (instability boundary intersects the $X$ axis) with an associated instability on the lower branch [here $g(X_L) > 0$ and $g(X_U) < 0$]. As $\Theta$ is increased, a second region of instability appears [Fig. 2(b)] corresponding to instability along the upper branch (Fig. 3). As $\Theta$ is increased further, the region of instability associated with bistability shrinks and eventually disappears, while the second instability remains [Figs. 2(c) and 2(d)]. This is a completely new instability, with no counterpart in the results reported for absorptive bistability.[1(c)]

## V. THE CASE $\Delta = -\Theta$

We give the case $\Delta = -\Theta$ special consideration, because with this restriction, we can obtain simple analytic instability conditions.

If we define

$$\tilde{Y} = \bar{Y}/(1+\Delta^2)^{1/2} = Y/(1+\Delta^2) \tag{38}$$

the state equation Eq. (18) becomes formally identical to the state equation for absorptive bistability:

$$\tilde{Y} = X\left[1 + \frac{2\bar{C}}{1+X^2}\right], \tag{39}$$

and we have the simple bistability condition

$$\bar{C} > 4, \tag{40a}$$

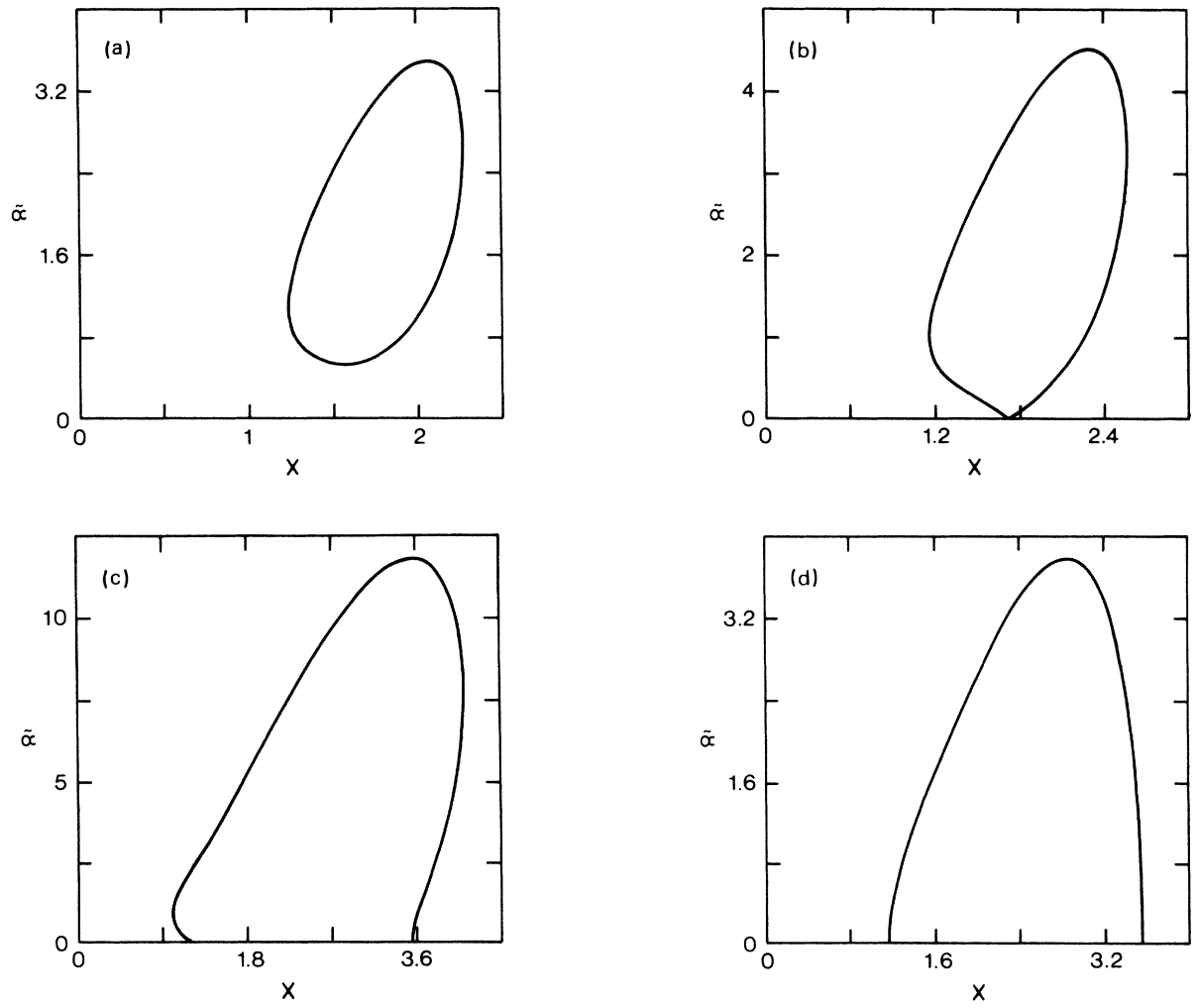


FIG. 4. Instability boundaries in the $(X,\tilde{\alpha})$ plane for (a) $\bar{C}=3.5$, $\Delta=2$, $\Theta=-2$; (b) $\bar{C}=4.0$, $\Delta=2$, $\Theta=-2$; (c) $\bar{C}=8.0$, $\Delta=2$, $\Theta=-2$; (d) $\bar{C}=8.0$, $\Delta=0.5$, $\Theta=-0.5$.

or, equivalently,

$$C > 1+\Delta^2 . \tag{40b}$$

Also, the condition $g(X)>0$ becomes

$$|\Delta| > 1 \tag{41}$$

and the condition $\mathscr{D}(X)\geq 1$ becomes

$$(1+\Delta^2)\frac{2\bar{C}X^2}{(1+X^2)^2} \geq 2|\Delta| \left[1+\frac{2\bar{C}}{(1+X^2)^2}\right] . \tag{42}$$

Since the requirement $g(X)>0$ is now independent of $X$, it follows that when bistability exists, if $|\Delta|>1$, then $g(X_L)>1$ and $g(X_U)>1$ so that there is a range of positive-slope instability on both the upper and lower branches as illustrated in Fig. 1. The extent of each unstable region in $X$ is determined by roots to the equation $\mathscr{D}(X_P)=0$, i.e., by solving Eq. (42) with the equals sign. This is a quadratic equation in $X_P$ and we find

$$(X_P^{1,2})^2 = \frac{\bar{C}(1+\Delta^2)}{2|\Delta|} - 1 \pm \frac{\bar{C}(1+\Delta^2)}{2|\Delta|} \times \left[1-\frac{4|\Delta|(1+|\Delta|)^2}{\bar{C}(1+\Delta^2)^2}\right]^{1/2} . \tag{43}$$

These are two real positive roots for

$$\bar{C} \geq \frac{4|\Delta|(1+|\Delta|)^2}{(1+\Delta^2)^2} . \tag{44}$$

For $|\Delta|>1$ and $\bar{C}>4$ Eq. (44) is always satisfied, as it must be by our observation that a positive-slope instability always accompanies bistability if $|\Delta|>1$. When $|\Delta|>1$ Eq. (44) is also satisfied for a range of $\bar{C}<4$, in which case positive-slope instability exists in the absence of bistability. This possibility has been reported previously by Lugiato.[13] Note that Eq. (43) gives all real positive roots for $X_P^2$ and therefore there can be no second instability as in Fig. 2 under the restriction $\Delta=-\Theta$. Indeed, it

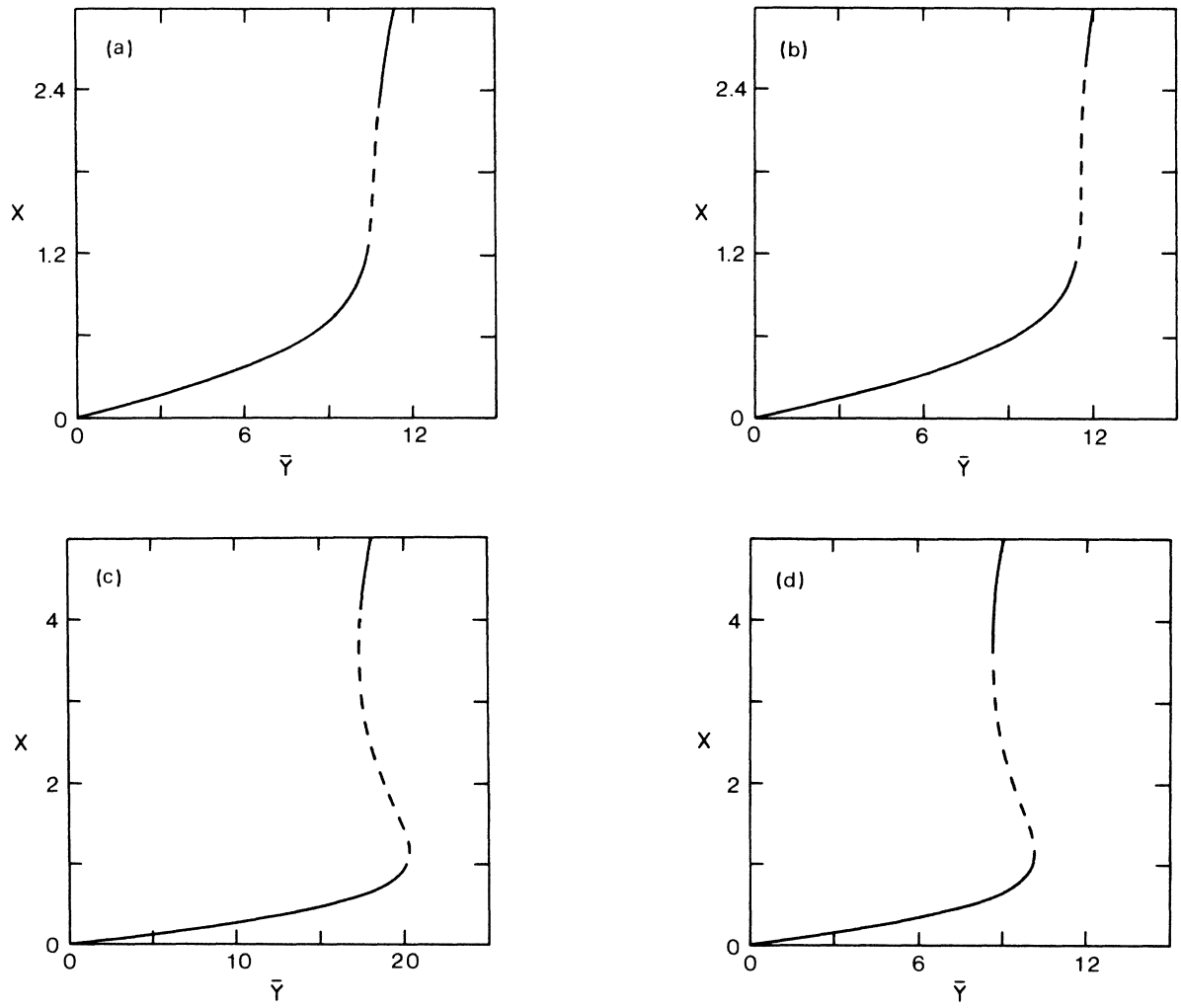


FIG. 5. Steady-state curves showing the unstable (dashed) regions corresponding to Figs. 4(a)—4(d), respectively.

can be shown that $\Delta$ and $\Theta$ must have the same sign for the second instability to exist.

We summarized results for instability boundaries with $\Delta=-\Theta$ in Figs. 4 and 5. It should be noted that the range of positive-slope instability given by $X_P^{1,2}$ and indicated in Fig. 5 corresponds to the projection of the unstable region in the $(X,\tilde{\alpha})$ plane onto the X axis and is generally not the range of instability for any fixed $\tilde{\alpha}$.

(1) For $|\Delta|>1$, $\bar{C}<4|\Delta|(1+|\Delta|)^2/(1+\Delta^2)^2$, and $|\Delta|<1$, $\bar{C}<4$, all steady states are stable.

(2) For $|\Delta|>1$, $4|\Delta|(1+|\Delta|)^2/(1+\Delta^2)^2<\bar{C}<4$, a region of the $(X,\tilde{\alpha})$ plane is unstable, but it does not intersect the X axis. A positive-slope instability exists in the absence of bistability [Figs. 4(a) and 5(a)].

(3) For $|\Delta|>1$, $\bar{C}=4$, a region of the $(X,\tilde{\alpha})$ plane is unstable and touches the X axis tangentially. A positive-slope instability exists at the onset of bistability [Figs. 4(b) and 5(b)].

(4) For $|\Delta|>1$, $\bar{C}>4$, a region of the $(X,\tilde{\alpha})$ plane is unstable and intersects the X axis at $X_L$ and $X_U$ with $g(X_L)<0$ and $g(X_U)<0$. Bistability exists together with positive-slope instabilities on both the lower and upper branches [Figs. 4(c) and 5(c)].

(5) For $|\Delta|<1$, $\bar{C}>4$, a region of the $(X,\tilde{\alpha})$ plane is unstable and intersects the X axis of $X_L$ and $X_U$ with $g(X_L)<0$ and $g(X_U)<0$. Bistability exists without a positive-slope instability [Figs. 4(b) and 5(d)].

## VI. NONLINEAR MODE EQUATIONS WITH ADIABATIC ELIMINATION OF THE POPULATION VARIABLES

We have found that for certain values of $\bar{C}$, $\Delta$, and $\Theta$, and an appropriate choice for $(\gamma_{\parallel}t_R)^{-1}$, all steady states can be unstable over some range of the incident field amplitude $\bar{Y}$ [for example, Figs. 3, 5(a), and 5(b)]. In such situations, the long-time behavior of the system necessarily evolves to undamped oscillations. Then in order to calculate the self-pulsing solution, we must return to the nonlinear mode equations [Eqs. (15)].

These equations are very complicated unless the number of modes taking part in the dynamics is small. In the resonant case $\Delta=\Theta=0$, it has been shown[22(b),22(c)] that when *only the first pair of off-resonant modes $n=\pm1$ are unstable*—i.e., when $|\tilde{\alpha}|=2\pi(\gamma_{\parallel}t_R)^{-1}$ lies in the unstable region of the $(X,\tilde{\alpha})$ plane, but $|\tilde{\alpha}|=2\pi|n|(\gamma_{\parallel}t_R)^{-1}$, $|n|>1$, does not—the dynamics can safely be restricted to the three modes $n=0,\pm1$. Here we assume that this also holds when $\Delta$ and $\Theta$ are nonzero. Then we drop all terms involving variables $f_n$ and $d_n$ with $|n|>1$ from Eqs. (15). Correspondingly, from Eqs. (13) and (14) we write

$$\bar{F}(z,t')=f_0(t')+f_1(t')\exp\left[-i\frac{2\pi}{t_R}\left[t'-\frac{z}{c}\frac{\mathscr{L}}{L}\right]\right]+f_{-1}(t')\exp\left[i\frac{2\pi}{t_R}\left[t'-\frac{z}{c}\frac{\mathscr{L}}{L}\right]\right], \tag{45}$$

where, from Eq. (8)

$$t'-\frac{z}{c}\frac{\mathscr{L}}{L}=t-\frac{z}{c}. \tag{46}$$

The dimensionless intensity is then

$$|\bar{F}(z,t')|^2=|f_0|^2+|f_1|^2+|f_{-1}|^2+2|f_0f_1^*+f_0^*f_{-1}|\cos\left[\frac{2\pi}{t_R}\left[t'-\frac{z}{c}\frac{\mathscr{L}}{L}\right]+\arg(f_0f_1^*+f_0^*f_{-1})\right]+2|f_1^*f_{-1}|\cos\left[\frac{4\pi}{t_R}\left[t'-\frac{z}{c}\frac{\mathscr{L}}{L}\right]+\arg(f_1^*f_{-1})\right]. \tag{47}$$

Note that since $\dot{f}_n\sim\kappa$, and $\kappa\ll2\pi t_R^{-1}$ in the mean-field limit, the terms $\arg(f_0f_1^*+f_0^*f_{-1})$ and $\arg(f_1^*f_{-1})$ contribute a negligible change to the beat frequency between empty cavity modes.

As in the linear stability analysis, we introduce the good-cavity limit [Eq. (21)] which allows us to eliminate adiabatically the population variables $d_n$. Again note that this is quite different from eliminating $D$ adiabatically in Eqs. (11). We simply set $\dot{d}_n=0$ in Eq. (15b) and solve for $d_n$ in terms of the more slowly varying $f_n$ and $f_n^*$. Adiabatic elimination of $D$ in Eqs. (11) corresponds to also setting $\tilde{\alpha}_n=0$. Then with $\dot{d}_n=0$ and truncation at $|n|=1$, from Eqs. (15) we obtain the following closed set of equations for $f_0,f_1,f_{-1}$ and their complex conjugates:

$$\dot{f}_0=\bar{Y}-[1+i\Theta+2\bar{C}(1-i\Delta)A]f_0-2\bar{C}(1-i\Delta)(Bf_1+B^*f_{-1}), \tag{48a}$$

$$\dot{f}_1=-[1+i\Theta+2\bar{C}(1-i\Delta)A]f_1-2\bar{C}(1-i\Delta)B^*f_0, \tag{48b}$$

$$\dot{f}_{-1}=-[1+i\Theta+2\bar{C}(1-i\Delta)A]f_{-1}-2\bar{C}(1-i\Delta)Bf_0, \tag{48c}$$

where

$$A=M^{-1}[(1+|f_0|^2+|f_1|^2+|f_{-1}|)^2+\tilde{\alpha}_1^2-|f_1^*f_{-1}|^2], \tag{49a}$$

$$B=-M^{-1}[(f_0f_1^*+f_0^*f_{-1})\times(1+|f_0|^2+|f_1|^2+|f_{-1}|^2-i\tilde{\alpha}_1)-(f_0f_1^*+f_0^*f_{-1})^*f_1^*f_{-1}], \tag{49b}$$

with

$$M=(1+|f_0|^2+|f_1|^2+|f_{-1}|^2)$$
$$\times[(1+|f_0|^2+|f_1|^2+|f_{-1}|^2)^2$$
$$+\tilde{\alpha}_1^2-|f_1^*f_{-1}|^2-2|f_0f_1^*+f_0^*f_{-1}|^2]$$
$$+2\,\mathrm{Re}[(f_0f_1^*+f_0^*f_{-1})^2(f_1^*f_{-1})^*]\,. \quad (50)$$

The equations for $f_0^*$, $f_1^*$, and $f_{-1}^*$ are given by the complex conjugates of Eqs. (48). The numerical solution of these six coupled equations will be discussed in a future paper.

## VII. LINEAR STABILITY ANALYSIS FOR A GAUSSIAN MODE

All of the foregoing analysis is for plane-wave fields. On the other hand, the incident laser beam has a transverse intensity profile that is typically Gaussian. Plane-wave conditions can only be met in experiments that use only the central portion of the beam. If this is not the experimental situation, it is important to investigate the effects of the transverse intensity profile on the instabilities we have been considering. Such an investigation is particularly important in the light of recent work which shows that self-pulsing in absorptive bistability can disappear completely after averaging over a Gaussian intensity profile.[26,27]

As in Ref. 26, we consider a ring cavity with spherical mirrors and an incident field matched to the $TEM_{00}$ mode in the presence of the atom-field interaction. This appears to be a reasonable approximation in the mean-field limit where self-focusing and self-defocusing effects are negligible, and if the Fresnel number of the cavity is low enough to provide sufficient diffractive mixing.[29] We assume that the Rayleigh length is larger than the length of the atomic sample so that the beam radius is practically constant over the sample length. Under these conditions, the dynamics of the system is governed by the single-transverse-mode model[30–32,26] where Eqs. (15) are replaced by

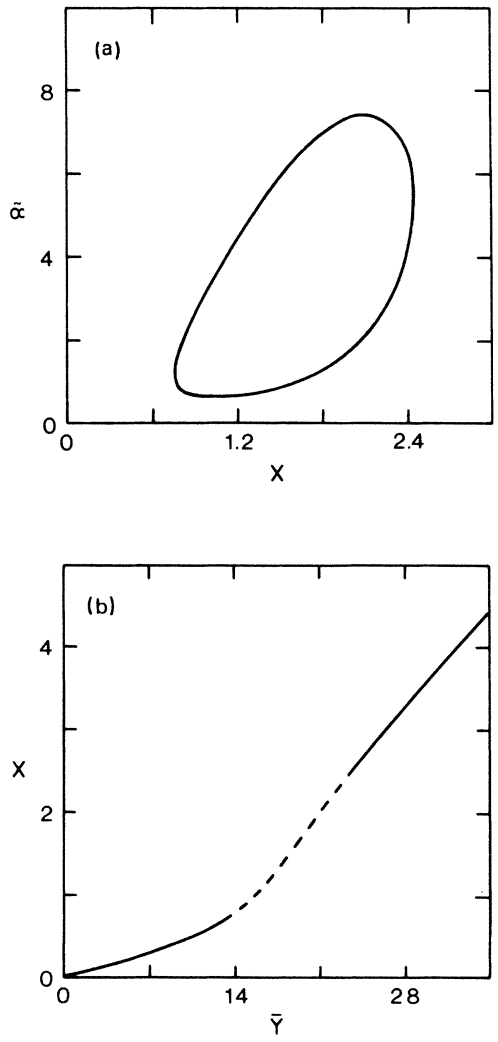


FIG. 6. (a) Instability boundary in the $(X,\tilde{\alpha})$ plane for $\bar{C}=1.2$, $\Delta=7$, $\Theta=-7$, from the plane-wave theory. (b) Corresponding steady-state curve showing the unstable (dashed) region.

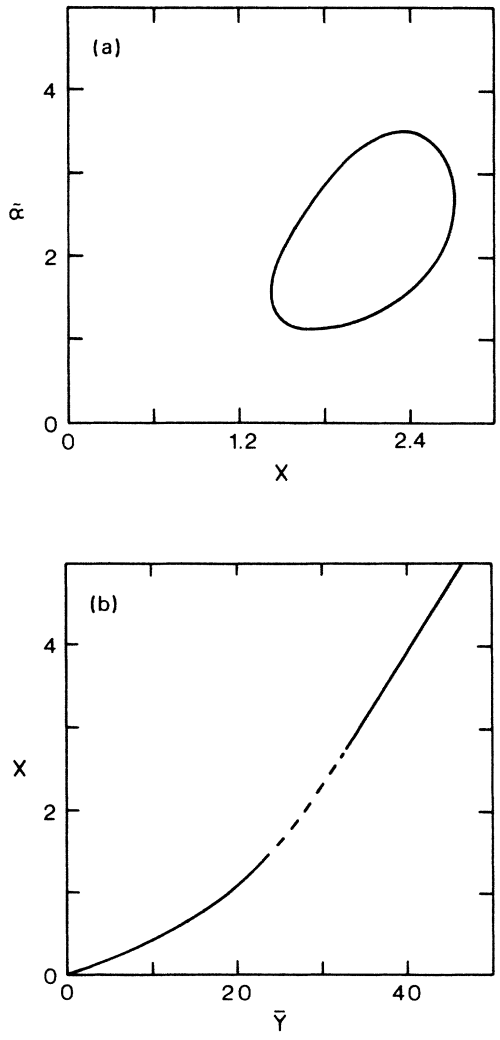


FIG. 7. Same as Fig. 6, but from the Gaussian mode theory.

$$\dot{f}_n = -\kappa \left[ (1+i\Theta) f_n + 2\bar{C}(1-i\Delta) \sum_{n'} f_{n'} \int_0^{d/W_0} dr\, 4re^{-2r^2} d_{n-n'}(r) - \bar{Y}\delta_{n,0} \right] , \tag{51a}$$

$$\dot{d}_n = i\tilde{\alpha}_n d_n - \gamma_{\parallel} \left[ d_n + e^{-2r^2} \sum_{n',n''} f_{n'}^* f_{n''} d_{n+n'-n''} - \delta_{n,0} \right] , \tag{51b}$$

where $W_0$ is the beam waist, $r$ is a dimensionless radial variable with $r=1$ at the beam waist, and $d$ is the radius of the cylindrical atomic sample. The field variables $f_n$ depend only on $t'$ while the population variables $d_n$ depend on both $t'$ and $r$. The steady-state solution which replaces Eqs. (16)—(18) now has the form

$$f_0^{(\mathrm{st})} = Xe^{i\phi_x} = X \left[ \frac{1-i\Theta+(2\bar{C}/X^2)(1+i\Delta)\ln[(1+X^2)/(1+\tilde{X}^2)]}{1+i\Theta+(2\bar{C}/X^2)(1-i\Delta)\ln[(1+X^2)/(1+\tilde{X}^2)]} \right]^{1/2} , \tag{52a}$$

$$d_0^{(\mathrm{st})}(r) = \frac{1}{1+X^2\exp(-2r^2)} , \tag{52b}$$

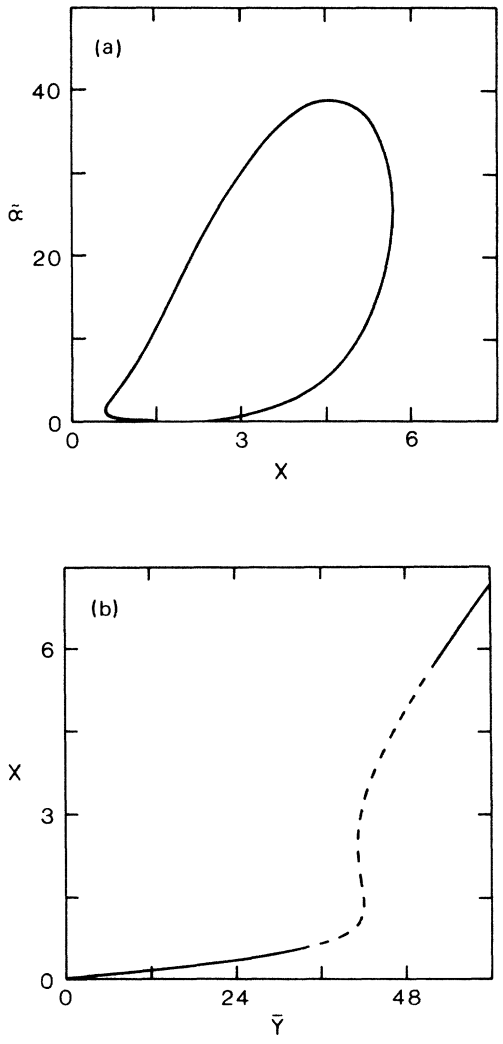


FIG. 8. (a) Instability boundary in the $(X,\tilde{\alpha})$ plane for $\bar{C}=4.8$, $\Delta=7$, $\Theta=-7$, from the plane-wave theory. (b) Corresponding steady-state curve showing the unstable (dashed) region.

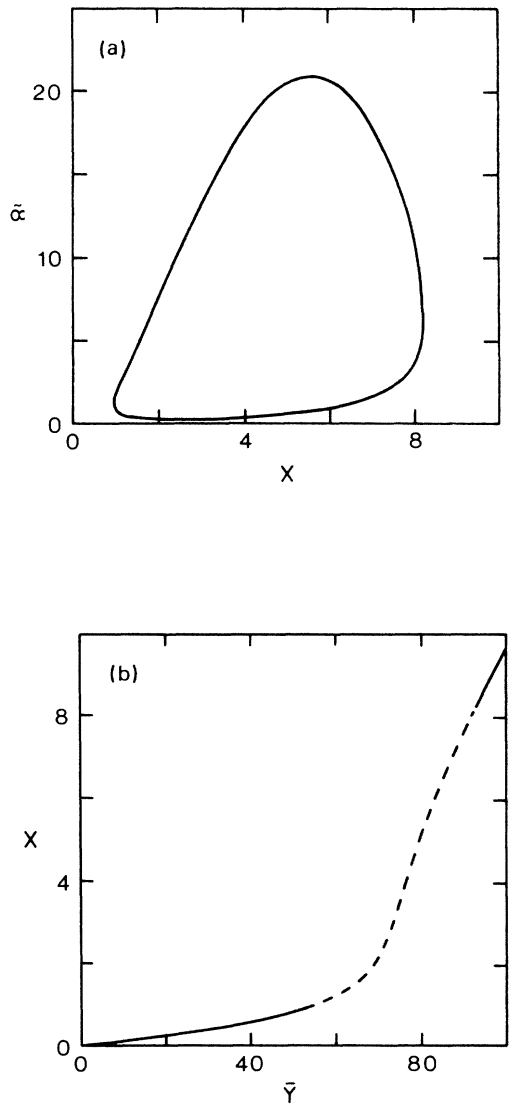


FIG. 9. Same as Fig. 8, but from the Gaussian mode theory.

where

$$\tilde{X}^2 = X^2 \exp\left[-2\left[\frac{d}{W_0}\right]^2\right], \tag{53}$$

and $|X| = |f_0^{(st)}|$ satisfies the state equation

$$\bar{Y} = X\left\{\left[1+\frac{2C}{X^2}\ln\left[\frac{1+X^2}{1+\tilde{X}^2}\right]\right]^2 + \left[\Theta - \frac{2\bar{C}\Delta}{X^2}\ln\left[\frac{1+X^2}{1+\tilde{X}^2}\right]\right]\right\}^{1/2}. \tag{54}$$

The linear stability analysis for the good-cavity limit [Eq. (21)] follows from Eqs. (51) in the same fashion as the plane-wave analysis of Eqs. (15). Here the eigenvalue equation, corresponding to Eq. (26), reads

$$\lambda_n^2 + 2\lambda_n(1+2\bar{C}\mathscr{A}) + 1 + \Theta^2 + 4\bar{C}^2(1+\Delta^2)(\mathscr{A}^2 - \mathscr{B}^2) + 4\bar{C}(1-\Delta\Theta)\mathscr{A} = 0, \tag{55}$$

where

$$\mathscr{A} = \frac{1}{X^2}\ln\left[\frac{1+X^2}{1+\tilde{X}^2}\right] + \mathscr{B}, \tag{56}$$

and

$$\mathscr{B} = \mathscr{B}_R + i\mathscr{B}_I \tag{57a}$$

with

$$\mathscr{B}_R = \frac{1}{X^2}\left[\frac{1}{2}\ln\left[\frac{1+X^2+\tilde{\alpha}_n^2}{1+\tilde{X}^2+\tilde{\alpha}_n^2}\right] + \frac{1}{\tilde{\alpha}_n}\tan^{-1}\left[\frac{(X^2-\tilde{X}^2)\tilde{\alpha}_n^2}{(1+X^2)(1+\tilde{X}^2)+\tilde{\alpha}_n^4}\right]\right], \tag{57b}$$

$$\mathscr{B}_I = \frac{1}{X^2}\left[\frac{1}{2\tilde{\alpha}_n}\ln\left[\frac{(1+X^2)}{(1+\tilde{X}^2)}\frac{(1+\tilde{X}^2)+\tilde{\alpha}_n^2}{(1+X^2)+\tilde{\alpha}_n^2}\right] - \tan^{-1}\left[\frac{(X^2-\tilde{X}^2)\tilde{\alpha}_n^2}{(1+X^2)(1+\tilde{X}^2)+\tilde{\alpha}_n^4}\right]\right]. \tag{57c}$$

As shown in Ref. 26, in the limit

$$\frac{d}{W_0}\to 0, \quad \bar{C}\to\infty \quad \text{with } \tilde{C} = 2\bar{C}\frac{d}{W_0} = \text{const} \tag{58}$$

the Gaussian mode theory reduces to the plane-wave theory with $\bar{C}$ replaced by $\tilde{C}$. Here we focus on the opposite limit $d/W_0\to\infty$. Our primary objective is to see whether positive-slope off-resonance-mode instabilities remain for this full Gaussian case.

Figures 6 and 7 and Figs. 8 and 9 compare the unstable region in the $(X,\tilde{\alpha})$ plane given by the plane-wave and Gaussian theories for two choices of $\bar{C}$, $\Delta$, and $\Theta$. In both cases, the positive-slope instability predicted by the plane-wave theory survives for a Gaussian mode. If we compare Figs. 8(a) and 9(a) we see that the unstable region has roughly the same area in both figures, but in Fig. 9 (Gaussian theory) it is more contracted in the $\tilde{\alpha}$ direction and extended in the $X$ direction. These features, and the fact that the instability persists here, whereas for $\Delta=\Theta=0$, $\gamma_{\parallel}\approx\gamma_{\perp}$, it disappears, can be understood on the basis of the following argument. For $d/W_0\to\infty$ ($\tilde{X}=0$) Eq. (55) is obtained from Eq. (26) by replacing $X$ by $\rho = X\exp(-2r^2)$ and performing the average

$$\frac{1}{X^2}\int_0^{X^2} d\rho\,.$$

Then when the unstable region of the $(X,\tilde{\alpha})$ plane for the

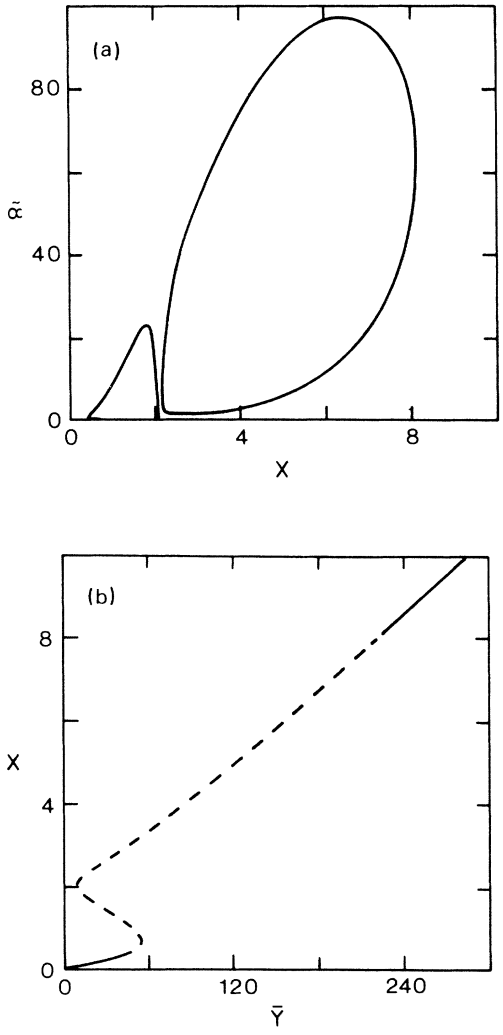


FIG. 10. (a) Instability boundary in the $(X,\tilde{\alpha})$ plane for $\bar{C}=8$, $\Delta=10$, $\Theta=30$, from the plane-wave theory. (b) Corresponding steady-state curve showing the unstable (dashed) region. Note that a small state region exists beyond the turning point on the upper branch which is not apparent in the figure.

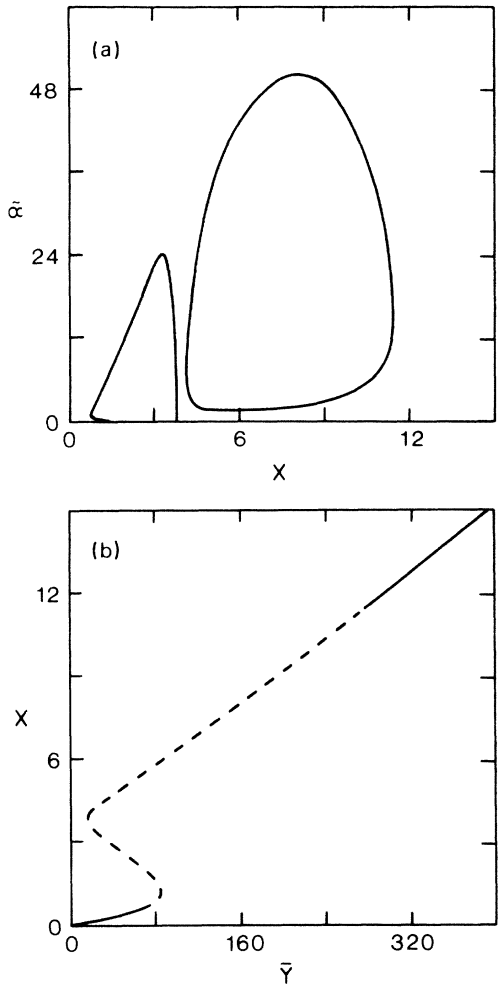


FIG. 11. Same as Fig. 10, but from the Gaussian mode theory.

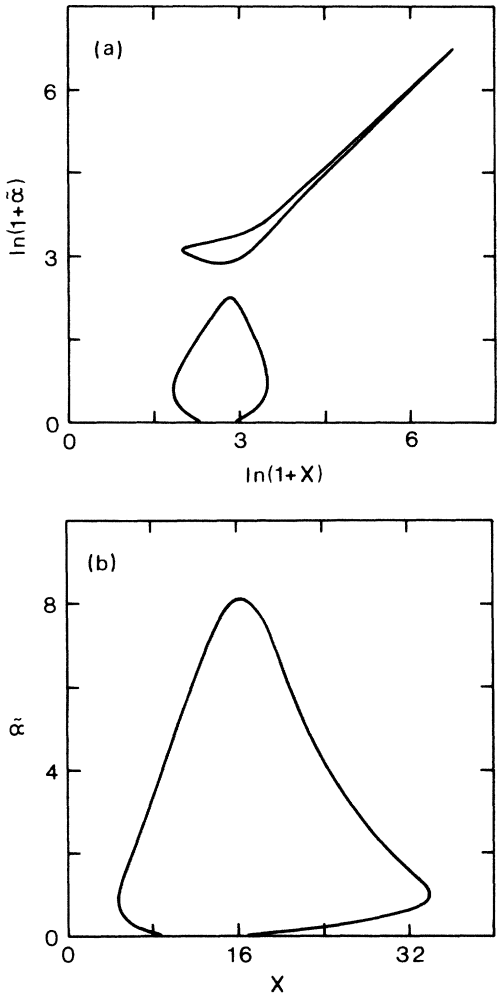


FIG. 12. Instability domain in the $(\tilde{\alpha},X)$ plane for $\bar{C}=4.8$, $\Delta=7$, $\Theta=-7$, $\gamma_{\parallel}=\gamma_{\perp}$.

plane-wave theory is narrow in the $X$ direction, under this averaging, the contribution from the range of $\rho$ over which Eq. (26) gives stable eigenvalues washes out the contribution from the small range of $\rho$ over which Eq. (26) gives an unstable eigenvalue. This is what happens for $\Delta=\Theta=0$, $\gamma_{\parallel}\approx\gamma_{\perp}$, where the positive-slope instability is associated with the narrow high-$\tilde{\alpha}$ end of the unstable region [see Refs. 1(c) and 11]. When the unstable region is broad in the $X$ direction, as it is here, the instability persists; the averaging can even extend the unstable region to larger values of $X$.

Finally, we must ask whether the new instability illustrated in Figs. 2 and 3 remains in the Gaussian theory. Adopting the same parameters as in Fig. 2, we find that it is absent. However, with the choice of different parameter values, Figs. 10 and 11 show that this instability is also preserved for a Gaussian mode.

## VIII. CONCLUDING REMARKS ON THE RATE-EQUATION APPROXIMATION

Our treatment has been restricted to the rate-equation limit [Eq. (10)]. We conclude with some results for $\gamma_{\parallel}=\gamma_{\perp}$ which show that we can expect similar instabilities when this limit is relaxed. Figure 12 shows the unstable region of the $(X,\tilde{\alpha})$ plane obtained from the results of Ref. 13 for $\gamma_{\parallel}=\gamma_{\perp}$. On comparison with Fig. 8(a), which is for the same values of $\bar{C}$, $\Delta$, and $\Theta$, note that both the lower-branch and upper-branch instabilities remain. A disconnected region of instability also appears which extends with a very long tail to high values of $X$ and $\tilde{\alpha}$. This is probably associated with the role of Rabi oscillations which are excluded in the rate-equation limit; in fact, this region is essentially centered around $\tilde{\alpha}=X$ which for $\gamma_{\parallel}=\gamma_{\perp}$ amounts to the statement that $\alpha$ is equal to the Rabi frequency of the internal field. Hence, the operating mechanism is different from that of the disconnected region in Figs. 2, 10, and 11 which only occurs when $\Delta$ and $\Theta$ have the same sign. Because of this long tail, Fig. 12(a) is plotted as $\ln(1+\tilde{\alpha})$ versus $\ln(1+X)$. If $\bar{C}$ is changed from 4.8 to 1.2, with all other parameters unchanged, the unstable region in Fig. 10 practically vanishes. Finally, without generalizing the stability analysis of Ref. 13 to a Gaussian mode, on the basis of the argument at the end of the last section, we can fairly safely say that the long nar-

row feature in Fig. 12 will be washed out by Gaussian averaging, while the lower region, shown in greater detail in Fig. 12(b), will remain.

We finally observe that the two disconnected domains in Fig. 12(a) appear to emerge from different instability mechanisms. The long-tailed part reminds us of the instability that is typical of the purely absorptive case,[3(b),4] i.e., it arises from the resonance between the Rabi frequency and the adjacent cavity modes. The other domain is similar to the instability domains found in this paper in the rate-equation approximation. This instability arises from the mismatch between the frequency of the input field, the nearest cavity mode, and the center of the atomic absorption line. This argument is especially clear if one considers the instability condition $g(\bar{C},\Delta,\Theta,X)>0$. For $X=\Theta=0$, $g$ is always negative. For $\Delta=0$ (or $\Theta=0$), it becomes positive if $|\Theta|$ (or $|\Delta|$) is made large enough. For $\Delta\neq 0$ and $\Theta\neq 0$, $g$ acquires its largest value when $\Delta$ and $\Theta$ have opposite signs. When $\Theta\Delta>0$, the instability appears only if the effects of $\Theta$ prevail over those of $\Delta$, as in Figs. 2(b)–2(d).

## ACKNOWLEDGMENTS

This research has been carried out in the framework of an operation launched by the Commission of the European Communities under the experimental phase of the European Community Stimulation Action. This work was supported in part by a NATO grant, by a grant from Research Corporation, by Consiglio Nazionale delle Ricerche, Contribution No. CT 83.00029.02, and by a contract from the U.S. Army Research Office.

[1](a) H. M. Gibbs, S. L. McCall, and T. N. C. Venkatesan, Opt. News **5**, 6 (1979); (b) E. Abraham and S. D. Smith, Rep. Prog. Phys. **45**, 815 (1982); (c) L. A. Lugiato, in *Progress in Optics*, edited by E. Wolf (North-Holland, Amsterdam, 1984), Vol. XXI, pp. 69–216.

[2]S. L. McCall, Appl. Phys. Lett. **32**, 284 (1978).

[3](a) R. Bonifacio and L. A. Lugiato, Lett. Nuovo Cimento **21**, 505 (1978); (b) **21**, 510 (1978).

[4](a) R. Bonifacio, M. Gronchi, and L. A. Lugiato, Opt. Commun. **30**, 129 (1979); (b) M. Gronchi, V. Benza, L. A. Lugiato, P. Meystre, and M. Sargent III, Phys. Rev. A **24**, 1419 (1981).

[5]K. Ikeda, Opt. Commun. **30**, 257 (1979).

[6]K. Ikeda, H. Daido, and O. Akimoto, Phys. Rev. Lett. **45**, 709 (1980).

[7]H. M. Gibbs, F. A. Hopf, D. L. Kaplan, and R. L. Shoemaker, Phys. Rev. Lett. **46**, 474 (1981); P. M. Petersen, J. N. Ravn, and T. Skettrup, Quantum Electron Lett., IEEE J. Quantum Electron. **QE-20**, 690 (1984).

[8]H. Nakatsuka, S. Asaka, H. Itoh, K. Ikeda, and M. Matsuoka, Phys. Rev. Lett. **50**, 109 (1983).

[9]R. G. Harrison, W. J. Firth, C. A. Emshary, and I. A. Al-Saidi, Phys. Rev. Lett. **51**, 562 (1983).

[10]L. A. Lugiato, M. L. Asquini, and L. M. Narducci, Opt. Commun. **41**, 450 (1982).

[11]H. J. Carmichael, Phys. Rev. Lett. **52**, 1292 (1984).

[12](a) J. A. Goldstone and E. M. Garmire, IEEE J. Quantum Electron. **QE-17**, 366 (1981); (b) H. G. Winful and G. D. Cooperman, Appl. Phys. Lett. **4B**, 298 (1982).

[13]L. A. Lugiato, Opt. Commun. **33**, 108 (1980).

[14]W. J. Firth, Opt. Commun. **30**, 343 (1981).

[15](a) R. R. Snapp, H. J. Carmichael, and W. C. Schieve, Opt. Commun. **40**, 68 (1981); H. J. Carmichael, R. R. Snapp and W. C. Schieve, Phys. Rev. A **26**, 3408 (1982); (c) H. J. Carmichael, in *Laser Physics*, Vol. 182 of *Lecture Notes in Physics*, edited by J. D. Harvey and D. F. Walls (Springer, Berlin, 1983) pp. 64–87; (d) J. C. Englund, R. R. Snapp, and W. C. Schieve, in *Progress in Optics*, edited by E. Wolf (North-Holland, Amsterdam, 1984), Vol. XXI, pp. 355–428.

[16]I. Bar-Joseph and Y. Silberberg, Opt. Commun. **48**, 53 (1983).

[17]K. Ikeda and O. Akimoto, Phys. Rev. Lett. **48**, 617 (1982).

[18]L. A. Lugiato, L. M. Narducci, D. K. Bandy, and C. A. Pennise, Opt. Commun. **43**, 281 (1982).

[19]L. A. Lugiato and L. M. Narducci, in *Coherence and Quantum Optics V*, edited by L. Mandel and E. Wolf (Plenum, New York, 1984), pp. 941–955.

[20]L. A. Lugiato, H. J. Horowicz, G. Strini, and L. M. Narducci, Phys. Rev. A **30**, 1366 (1984).

[21]L. A. Orozco, A. T. Rosenberger, and H. J. Kimble, Phys. Rev. Lett. **53**, 2547 (1984).

[22]L. A. Lugiato, Z. Phys. **41**, 85 (1981).

[23]L. A. Lugiato, Phys. Rev. A **28**, 483 (1983).

[24](a) V. Benza and L. A. Lugiato, Z. Phys. B **35**, 383 (1979); (b) Z. Phys. **47**, 79 (1982); (c) V. Benza, L. A. Lugiato, L. M. Narducci, and J. D. Farina, Z. Phys. **49**, 351 (1983).

[25](a) H. Haken, Z. Phys. B **21**, 105 (1975); (b) **22**, 73 (1975).

[26]L. A. Lugiato and M. Milani, Z. Phys. B **50**, 171 (1983).

[27]S. Stuut and M. Sargent III, J. Opt. Soc. Am. B **1**, 95 (1984).

[28]D. Armbruster, Z. Phys. B **53**, 157 (1983).

[29]This claim is confirmed by the very good quantitative agreement between experiment and single-mode Gaussian theory for steady-state bistability with two-level atoms; see A. T. Rosenberger, L. A. Orozco, and H. J. Kimble, Phys. Rev. A **28**, 2569 (1983); and in *Fluctuations and Sensitivity in Nonequilibrium Systems*, edited by W. Horsthemke and D. K. Kondepudi (Springer, Berlin, 1984), pp. 62–69.

[30]R. J. Ballagh, J. Cooper, M. W. Hamilton, W. J. Sandle, and D. M. Warrington, Opt. Commun. **37**, 143 (1981).

[31]P. D. Drummond, IEEE J. Quantum Electron. **QE-17**, 301 (1981).

[32]A. Gozzini, F. Maccarrone, and I. Longo, Nuovo Cimento D **1**, 489 (1982).